ChemPubSoc Europe

DOI: 10.1002/cctc.201701897

CHEMCATCHEM Communications

Porous Carbon Nanosheet-Supported Chiral Squaramide for Highly Enantioselective Friedel–Crafts Reaction

Liyuan Zhao,[a] Xiaoze Bao,[b] Qingtao Hu,[a] Baomin Wang,*[b] and An-Hui Lu*[a]

Porous carbon nanosheets (PCNs) were used for the first time as a support to immobilize a quinine–squaramide catalyst for the asymmetric Friedel–Crafts addition of pyrazolones to isatin ketimines. Relying on its open structure with a macroporous network as well as hydrophobicity, the PCN-supported catalyst presented catalytic performance comparable to its homogeneous catalyst; the products were obtained in high yields (up to 90%) with high *ee* values (up to 99%). Recycling batch reactions together with a continuous flow process confirmed the stability of the catalyst.

The heterogenization of homogeneous chiral catalysts is considered an effective approach towards sustainable asymmetric synthesis.[1] This strategy can provide easily recyclable solid catalysts with clearly known active sites similar to their homogeneous counterparts. Nevertheless, heterogenized chiral catalysts achieved by the surface covalent tethering strategy usually exhibit poor enantioselectivity owing to limited free space for chiral induction[2] and uncontrolled activity owing to certain side reactions initiated by the supports. Hence, the structural features and physicochemical properties of catalyst support materials are critical to determine the performance of heterogenized catalysts.

To date, silica-based porous materials have been extensively studied for immobilizing chiral molecular catalysts, as their abundant surface hydroxy groups allow the easy grafting of molecules by silylation.[3] Silica materials with inherent silanol groups have also been used as components of acid–base synergic catalysts, which facilitate some reaction processes with good activity;[4] however, their hydrothermal instability, poor resistance to acidic and basic media, and the acidic nature of their surface silanol groups, which could allow undesirable reactions, may restrict their compatibility in a number of reaction systems.[5] On the other hand, a wide range of organic polymers have also been examined as heterogeneous supports.[6] Owing to the intrinsic solubility of some linear and dendritic polymers, additional solvents need to be used as precipitants to recover soluble polymer catalysts.[7] Additionally, insoluble polymers endow catalysts with recyclability by simple filtration or centrifugation, and in some cases, the supported catalysts can work well in fixed-bed reactors,[6c,d,8] which, however, may lead to a high pressure drop as a result of the swelling effect. Recently, porous carbon materials have attracted great attention for their wide applications.[9] Relying on their good thermal and chemical stability, porous carbons are a vital type of solid support,[10] as they may be resistant to structural changes caused by hydrolytic or swelling effects in the reaction media.[11] Generally, the surface of porous carbons is relatively chemically inert, which is preferable for some catalytic systems, such as the hydrogen-bonding-promoted process in asymmetric chemistry. Through specific chemical modification of their surface π-conjugated systems, various molecular catalysts can be grafted on the surface of porous carbons.[12] Distinguished from other hydrophilic inorganic supports, porous carbons have great affinity to organic molecules and, therefore, can concentrate substrates near the catalytic active sites, which will probably accelerate the reaction rate. Hence, the utilization of porous carbons as a candidate to immobilize chiral catalysts and to explore their catalytic applications holds great potential.

Porous carbon nanosheets (PCNs), which are characterized by the existence of two-dimensional units, possess naturally open and interconnected macropores (Figure 1).[13] In this sense, they can afford free space not only for facilitating mass transport but also for good retention of the original chiral environment if chiral molecular catalysts are immobilized on the PCNs. In view of these general merits of PCNs, they may have the potential to act as an ideal support for immobilizing chiral molecular catalysts. Moreover, the multicompartment-like structure resulting from stacks of nanosheet units seems similar to a microreactor, which could possibly increase the local

[a] L. Y. Zhao, Q. T. Hu, Prof. Dr. A.-H. Lu
State Key Laboratory of Fine Chemicals,
School of Chemical Engineering
Dalian University of Technology
Dalian 116024 (P.R. China)
E-mail: anhuilu@dlut.edu.cn

[b] X. Z. Bao, Prof. Dr. B. M. Wang
State Key Laboratory of Fine Chemicals,
School of Pharmaceutical Science and Technology
Dalian University of Technology
Dalian 116024 (P.R. China)
E-mail: bmwang@dlut.edu.cn

Supporting Information for this article can be found under: https://doi.org/10.1002/cctc.201701897.

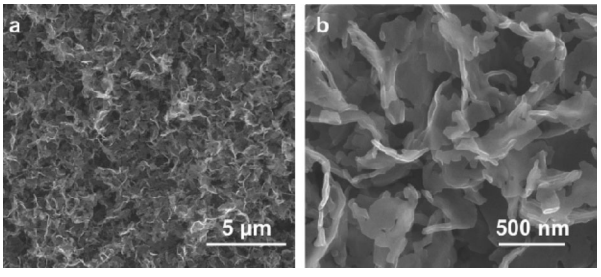

Figure 1. FESEM images of the porous carbon nanosheets at a) low and b) high magnification.

concentration of substrate molecules and thus accelerate the reaction process, finally exhibiting homogeneous-like activity. To our best knowledge, PCN-grafted chiral catalysts have not yet been reported.

In this work, we report the first example of PCN-supported quinine-based squaramide catalysts and their catalytic performance for the asymmetric Friedel–Crafts addition of pyrazolones to isatin ketimines. In accord with our expectations, the PCN-immobilized asymmetric catalysts showed homogeneous-like catalytic performance, and the optimal PCN-supported catalyst (PCN-Q1-1, Scheme 1) could be effectively recycled in batch and flow reactions.

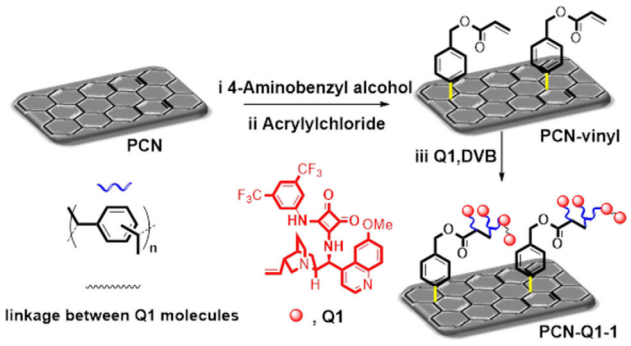

Scheme 1. Schematic structure of the designed PCN-supported catalysts.

The PCNs possess a surface area of 576 $m^2 g^{-1}$ and micropores mainly distributed around 0.6 nm. More importantly, they have interconnected macropores ranging from 300 nm to 1 μm, as measured by the mercury-injection test (Figure S1 in the Supporting Information), which make them a favorable support for grafting a relatively large-sized quinine-based squaramide catalyst (Q1). Relying on fused rings with sp^2 carbon atoms of the PCN surface, free-radical addition by diazonium chemistry[14] was employed to anchor the functional groups. This method, conducted under mild conditions, keeps the PCN surface inert, which outperforms the strategy of surface oxidation by nitric acid or dichromate. As outlined in Scheme 1, the PCNs were covalently bonded with the diazonium salt formed in situ from 4-aminobenzyl alcohol and sodium nitrite to obtain 4-hydroxymethylphenyl-functionalized PCN (PCN-BnOH; Bn = benzyl), and then the latter was condensed with acryloyl chloride to give the vinyl-functionalized PCN intermediate (PCN-vinyl). Finally, free-radical polymerization of PCN-vinyl with Q1 afforded the PCN-supported catalyst (PCN-Q1-1), for which divinylbenzene (DVB) was used as a linker. It is well recognized that mobility of the active sites in solid catalysts favors catalytic performance.[15] Hence, the DVB linker involved here was supposed to increase the flexibility of the polymeric chains and to decrease the inferior crowding trend among the Q1 molecules. For comparison, the PCN-supported catalyst prepared without the addition of DVB (PCN-Q1-2) was synthesized following the same procedure.

The IR spectrum of PCN-vinyl (Figure 2a) demonstrates the successful attachment of the vinyl group to the PCNs, as evidenced by the –COO– stretch at $\tilde{\nu} = 1720\ cm^{-1}$. The band at $\tilde{\nu} \approx 1600\ cm^{-1}$ is assigned to C=C stretching vibrations, mainly from the PCN aromatic skeleton. The adjacent bands ranging from $\tilde{\nu} = 1500$ to 1090 cm^{-1} are for the C–N and C–O stretching vibrations of the PCNs.[16] Raman spectroscopy was also used to validate the covalent nature of the immobilization. After two-step chemical modification, PCN-vinyl showed an increase in the Raman ratio of the areas of the D and G bands (A_D/A_G) to 1.68 (Table S1) upon using pristine PCNs as a reference (Raman $A_D/A_G = 1.34$); this is consistent with the formation of a new aryl–PCN bond. Incorporation of the Q1 active species on the PCN support was proved by solid-state ^{19}F magic-angle spinning (MAS) NMR spectroscopy (Figure 2b). PCN-Q1-1 produced a fluorine signal at $\delta = -62.4$ ppm, which corresponds to the trifluoromethyl ($-CF_3$) moiety of Q1. Consequently, this grafting method afforded 6.5 wt% of Q1 from PCN-Q1-1, as determined by elemental analysis (Table S2 and calculations for the Q1 content).

Quinine-based squaramide catalophore is an effective bifunctional hydrogen-bond-donor catalyst[17] that outperforms the corresponding thiourea analogues in the asymmetric Friedel–Crafts addition of pyrazolones to isatin ketimines, as we re-

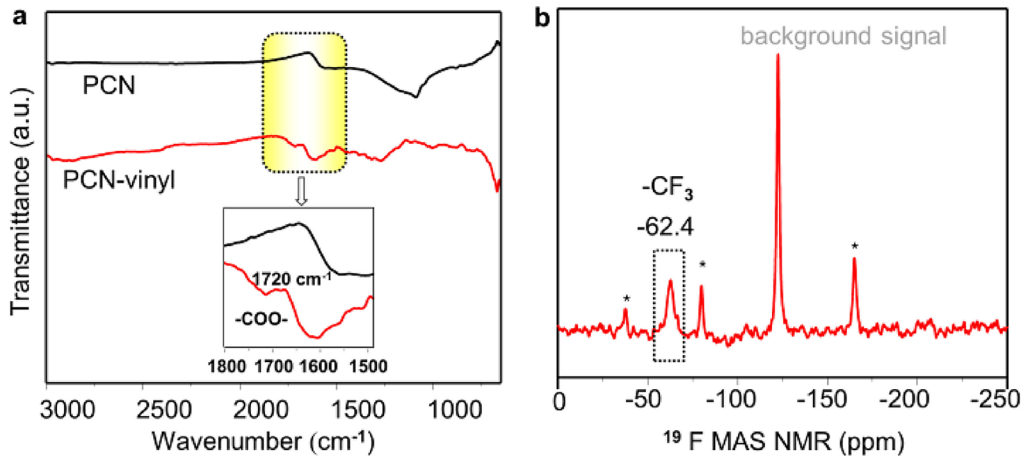

Figure 2. a) FTIR spectra of PCN and PCN after functionalization with vinyl (PCN-vinyl). b) Solid-state ^{19}F MAS NMR spectrum of PCN-Q1-1; signals corresponding to the asterisks are the spinning sidebands.

cently reported.[18] The oxindole–pyrazolone conjugates have 3-substitued-3-aminooxindoles motifs, which constitute the core structure of numerous natural products and drug candidates.[19] In this study, we first evaluated the performance of the prepared heterogeneous catalysts (PCN-Q1-1 and PCN-Q1-2) in the enantioselective addition of pyrazolone **2a** to isatin ketimine **1a**. To our delight, both PCN-Q1-1 and PCN-Q1-2 were highly active, and they both catalyzed the reaction to afford product **3** in high yields with high *ee* values (Table 1, entries 2 and 3). PCN-Q1-1 showed better activity than PCN-Q1-2, and the catalytic performance of the former was found to be comparable to that of the homogeneous catalyst Q1 (Table 1, entry 10). PCN-Q1-1 provided the product with *ee* values greater than 99% and high diastereoselectivities over 20:1 dr. The fact that the enantioselective performances are comparable strongly indicates that the Q1 molecules grafted on PCN through the DVB molecular linker, which increases the space distance, inherit the mobility and original chiral environment of the homogeneous analogue (Q1). However, in the case of the PCN-Q1-2 catalyst, the Q1 molecules without the DVB linker underwent self-polymerization. This limited space mobility may lead to slightly lower enantioselectivity. In contrast to our immobilized catalysts, the blank run with only PCN gave low activity and no enantioselectivity (Table 1, entry 1), which proved that the performance of our catalysts mainly resulted from grafted Q1. In addition, as demonstrated in our previous work,[18] the enantioselectivity stemmed from Q1 in the first step and is independent of the fluorination in the second step.

Table 1. Asymmetric Friedel–Crafts addition of pyrazolone **2a** to isatin-derived *N*-Boc ketimine oxindole **1a** with different catalysts.[a]

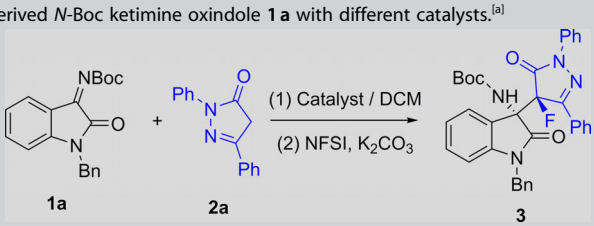

Entry	Catalyst	Time[b] [min]	Yield[c] [%]	*ee*[d] [%]
1	PCN	15	25	0
2	PCN-Q1-1	15	94	>99
3	PCN-Q1-2	15	90	93
4	SiO_2-Q1-1	120	89	40
5	SiO_2	120	80	0
6	AC-Q1-1	70	90	85
7[e]	PCN + Q1	15	94	>99
8[f]	PCN + $Q1^{2th}$	15	73	67
9[f]	PCN + $Q1^{3th}$	15	49	14
10[g]	Q1	20	94	>99

[a] Reaction conditions: catalyst (12 mg), PCN-Q1-1 (Q1 loading of 0.78 mg, 2 mol%), **1a** (0.06 mmol), **2a** (0.07 mmol), K_2CO_3 (0.09 mmol), and NFSI (0.09 mmol), CH_2Cl_2 as solvent (1 mL) at 25 °C; total reaction time of 2.5 h. [b] Time for the first step. [c] Yield of isolated product. [d] The *ee* value was determined by chiral-phase HPLC analysis. [e] The catalyst was a mixture of PCN (12 mg) and Q1 (1 mg). [f] The catalyst (mixture of PCN and Q1) was recycled from the last run by centrifugation and was washed with CH_2Cl_2 (3×). [g] The result was derived from Ref. [18], and the dosage of homogeneous catalyst Q1 was 2 mol%.

Then, the recyclability of PCN-Q1-1 was investigated. The immobilized catalyst could be easily recycled through a centrifugation process, and after five consecutive recycles, it still afforded target product **3** in 90% yield with 98% *ee* (Figure S5a). This excellent stability was evidenced by ^{19}F MAS NMR characterization of recycled PCN-Q1-1, which revealed no changes in the chemical shift of the trifluoromethyl (–CF_3) group from Q1 (Figure S4). Moreover, to test the stability of the catalyst, the filtrate from the solution of PCN-Q1-1 soaked in CH_2Cl_2 was used as the reaction medium. As a result, only 20% yield of **3** was obtained with no *ee* value. To understand further the stability of covalently bonded PCN-Q1-1, a physical mixture of PCN and Q1 was used as another control catalyst in this reaction. After three runs of the physical mixture (Table 1, entries 7–9), the yield and *ee* value of **3** dramatically decreased to 49% and 14%, respectively; these values are much lower than those obtained with PCN-Q1-1 (Figure S5b) and implied that the Q1 molecules leached out from the PCN support easily without covalent-bond tethering. The control experiment indicated that the strong covalent bonds between Q1 and the PCN support were critical to maintain the stability of PCN-Q1-1 in a highly active catalytic process without eroding the enantioselectivity.

Driven by the curiosity of the effect of the support, a silica-immobilized Q1 catalyst (SiO_2-Q1-1) was synthesized and examined. As displayed in entry 4 (Table 1), SiO_2-Q1-1 required a longer time to accomplish the first reaction step, affording a modest *ee* value of 40%, although the amount of grafted Q1 exposed on the SiO_2 surface was equal to or even more than that exposed on the PCN surface [X-ray photoelectron spectroscopy (XPS) characterization, Table S4 and Figure S8]. The behavior of SiO_2-Q1-1 indicates that porous silica, which is a hydrophilic inorganic support, is relatively incompatible with organic compounds and thus has lower reaction efficiency than the carbon-based catalyst. The poor stereocontrol of SiO_2-Q1-1 can possibly be attributed to surface Si–OH groups, which lead to partial background reactions and erode the enantioselectivity. This result was also confirmed by another control experiment performed with SiO_2 that mediated the conversion of substrates **1a** and **2a** into the product with no *ee* value (Table 1, entry 5). In addition, for better understanding of the support effects, an activated-carbon-based catalyst (AC-Q1-1) was also prepared and evaluated. AC-Q1-1 catalyzed the reaction between **1a** and **2a** with a longer time and provided product **3** with a lower *ee* value than that resulting from the use of PCN-Q1-1 (Table 1, entry 6). The surface oxygen groups from the edge sites of the activated carbon, which could form hydrogen bonds with the substrates, may erode the enantioselectivity and activity of the catalytic active sites.[20] The above results demonstrate that PCNs are preferred over porous silica and activated carbon in this hydrogen-bonding-promoted process as a porous carbon support owing to its hydrophobicity and chemical inertness.

With regard to the good performance of PCN-Q1-1, the scope of the reaction with typical substrates **4**–**7** was further

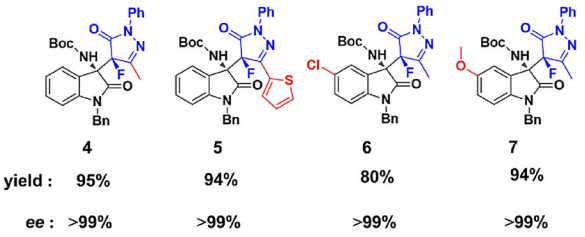

Figure 3. Scope of the Friedel–Crafts addition/fluorination sequence; dr > 20:1 in all cases. Bn = benzyl.

studied (Figure 3). Methyl and thienyl substituents at the C3 position of the pyrazolone ring were well accommodated, and products **4** and **5** were obtained in outstanding yields up to 90% with *ee* values greater than 99%. *N*-Boc ketimines (Boc = *tert*-butoxycarbonyl) with chloro and methoxy substituents on the benzene ring were also competent substrates, and products **6** and **7** were obtained in similar yields with almost the same levels of stereoselectivity as those afforded by the parent homogeneous catalyst Q1. The high catalytic efficiency of PCN-Q1-1 reflects that Q1 appended onto the PCNs is fully exposed to the reaction medium and gives rise to a homogeneous-like catalytic environment for the active sites.

To gain better insight into the nature of PCN-Q1-1, a continuous-flow process with a two-pump system (Figure 4) was performed. The packed-bed reactor filled with PCN-Q1-1 was fed with two solutions containing substrates **1a** and **2a** for the asymmetric Friedel–Crafts addition (step I). Then, the downstream of step I and *N*-fluorobenzenesulfonimide (NFSI) were simultaneously pumped into the K_2CO_3 column to give target product **3**. Under these conditions, the flow reaction was run for 6 h, after which time **3** (478 mg) was isolated with a productivity of 0.7 mmol h^{-1} $g_{PCN\text{-}Q1\text{-}1}{}^{-1}$ (91% yield, 88% *ee*). There was no detectable decrease in the catalytic activity of PCN-Q1-1 during the run time. However, the *ee* value was lower than that in batch. We therefore propose that after substrates **1a** and **2a** are pumped into the packed-bed reactor (step I), they may react with each other spontaneously before they diffuse into the catalytic sites, which would result in low enantioselectivity. Nevertheless, this continuous-flow experiment essentially

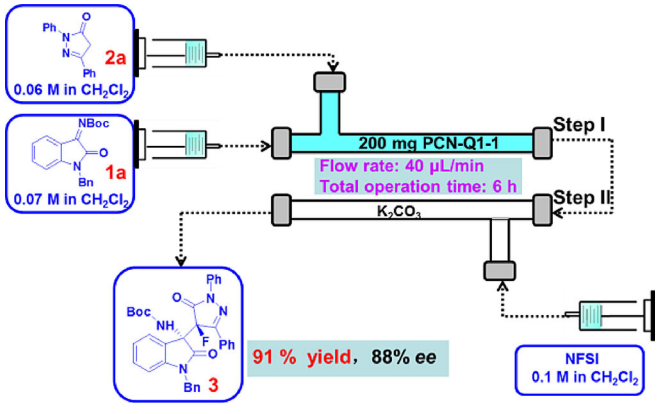

Figure 4. Experimental setup for the continuous-flow asymmetric Friedel–Crafts addition/fluorination sequence.

demonstrated the reusability and stability of the heterogenized chiral catalysts.

In summary, porous carbon nanosheet (PCN)-grafted quinine–squaramide catalysts with open and interconnected macropores were designed and synthesized for the efficient asymmetric Friedel–Crafts addition of pyrazolones to isatin ketimines. With divinylbenzene as a linker, the catalytic performance of the PCN-supported catalyst was comparable to that of its corresponding homogeneous analogue, and it afforded the products in yields greater than 90% with 99% *ee*. This catalyst also outperformed porous-silica- and activated-carbon-supported catalysts as a result of the hydrophobicity and chemical inertness of the PCNs. Moreover, the PCN-grafted quinine–squaramide worked efficiently over five recycling batch reactions as well as in a continuous-flow process. Our developed strategy of covalently immobilizing a chiral squaramide on PCNs holds great potential for designing other immobilized chiral catalysts for highly effective asymmetric reactions.

Acknowledgements

This work was financially supported by the National Natural Science Foundation of China (No. 21473021) and Cheung Kong Scholars Programme of China (T2015036).

Conflict of interest

The authors declare no conflict of interest.

Keywords: asymmetric catalysis · heterocycles · heterogeneous catalysis · nanostructures · supported catalysts

[1] H.-U. Bluser, B. Pugin, M. Studer in *Chiral Catalyst Immobilization and Recycling* (Eds.: D. E., De Vos. I. F., Vankelecom, P. A., Jacobs), Wiley-VCH, Weinheim, **2008**, pp. 1–15.
[2] A. E. C. Collis, I. T. Horváth, *Catal. Sci. Technol.* **2011**, *1*, 912–919.
[3] a) H. Zou, S. S. Wu, J. Shen, *Chem. Rev.* **2008**, *108*, 3893–3957; b) S. Minakata, M. Komatsu, *Chem. Rev.* **2009**, *109*, 711–724.
[4] a) S. S. Wang, J. He, Z. An, *Chem. Commun.* **2017**, *53*, 8882–8885; b) S. Shylesh, A. Wagener, A. Seifert, S. Ernst, W. R. Thiel, *Angew. Chem. Int. Ed.* **2010**, *49*, 184–187; *Angew. Chem.* **2010**, *122*, 188–191.
[5] a) R. P. Ye, L. Lin, J. X. Yang, M. L. Sun, F. Li, B. Li, Y. G. Yao, *J. Catal.* **2017**, *350*, 122–132; b) K. Sakthivel, W. Notz, T. Bui, C. F. Barbas III, *J. Am. Chem. Soc.* **2001**, *123*, 5260–5267.
[6] a) J. N. Lu, P. H. Toy, *Chem. Rev.* **2009**, *109*, 815–838; b) A. B. Powell, Y. Suzuki, M. Ueda, C. W. Bielawski, A. H. Cowley, *J. Am. Chem. Soc.* **2011**, *133*, 5218–5220; c) I. Sagamanova, C. Rodríguez-Escrich, I. G. Molnár, S. Sayalero, R. Gilmour, M. A. Pericás, *ACS Catal.* **2015**, *5*, 6241–6248; d) L. Clot-Almenara, C. Rodríguez-Escrich, L. Osorio-Planes, M. A. Pericás, *ACS Catal.* **2016**, *6*, 7647–7651; e) V. B. Saptal, B. M. Bhanage, *ChemCatChem* **2016**, *8*, 244–250.
[7] a) M. I. Burguete, J. M. Fraile, J. Garcıa, E. García-Verdugo, S. V. Luis, J. A. Mayoral, *Org. Lett.* **2000**, *2*, 3905–3908; b) A. Rolland, D. Hérault, F. Touchard, C. Saluzzo, R. Duval, M. Lemaire, *Tetrahedron: Asymmetry* **2001**, *12*, 811–815.
[8] D. Ragno, G. D. Carmine, A. Brandolese, O. Bortolini, P. P. Giovannini, A. Massi, *ACS Catal.* **2017**, *7*, 6365–6375.
[9] C. D. Liang, Z. J. Li, S. Dai, *Angew. Chem. Int. Ed.* **2008**, *47*, 3696–3717; *Angew. Chem.* **2008**, *120*, 3754–3776.
[10] a) S. H. Joo, S. J. Choi, I. Oh, J. Kwak, Z. Liu, O. Terasaki, R. Ryoo, *Nature* **2001**, *412*, 169–172; b) Q. N. Wang, L. Shi, A.-H. Lu, *ChemCatChem*

2015, *7*, 2846 – 2852; c) Z. L. Li, J. H. Liu, C. G. Xia, F. W. Li, *ACS Catal.* **2013**, *3*, 2440 – 2448; d) S. Jun, M. Choi, S. Ryu, H. Y. Lee, R. Ryoo, *Stud. Surf. Sci. Catal.* **2003**, *146*, 37 – 40; e) H. Yang, S. J. Bradley, A. Chan, G. I. N. Waterhouse, T. Nann, P. E. Kruger, S. G. Telfer, *J. Am. Chem. Soc.* **2016**, *138*, 11872 – 11881.

[11] a) J. Lee, J. Kim, T. Hyeon, *Adv. Mater.* **2006**, *18*, 2073 – 2094; b) S. Xin, Y. G. Guo, L. J. Wan, *Acc. Chem. Res.* **2012**, *45*, 1759 – 1769; c) Z. Y. Jin, Y. Y. Xu, Q. Sun, A.-H. Lu, *Small* **2015**, *11*, 5151 – 5156; d) D. Qian, C. Lei, E. M. Wang, W. C. Li, A.-H. Lu, *ChemSusChem* **2014**, *7*, 291 – 298; e) G. P. Hao, W. C. Li, D. Qian, G. H. Wang, W. P. Zhang, T. Zhang, A. Q. Wang, F. Schüth, H.-J. Bongard, A.-H. Lu, *J. Am. Chem. Soc.* **2011**, *133*, 11378 – 11388.

[12] a) A. Stein, Z. Y. Wang, M. A. Fierke, *Adv. Mater.* **2009**, *21*, 265 – 293; b) A. Faghani, I. S. Donskyi, M. F. Gholami, B. Ziem, A. Lippitz, W. E. S. Unger, C. Böttcher, J. P. Rabe, R. Haag, M. Adeli, *Angew. Chem. Int. Ed.* **2017**, *56*, 2675 – 2679; *Angew. Chem.* **2017**, *129*, 2719 – 2723.

[13] G. P. Hao, Z. Y. Jin, Q. Sun, X. Q. Zhang, J. T. Zhang, A.-H. Lu, *Energy Environ. Sci.* **2013**, *6*, 3740 – 3747.

[14] a) J. L. Bahr, J. P. Yang, D. V. Kosynkin, M. J. Bronikowski, R. E. Smalley, J. M. Tour, *J. Am. Chem. Soc.* **2001**, *123*, 6536 – 6542; b) A. Schätz, R. N. Grass, W. J. Stark, O. Reiser, *Chem. Eur. J.* **2008**, *14*, 8262 – 8266; c) D. Dasler, R. A. Schafer, M. B. Minameyer, J. F. Hitzenberger, F. Hauke, T. Drewello, A. Hirsch, *J. Am. Chem. Soc.* **2017**, *139*, 11760 – 11765.

[15] Q. Sun, Z. F. Dai, X. L. Liu, N. Sheng, F. Deng, X. J. Meng, F.-S. Xiao, *J. Am. Chem. Soc.* **2015**, *137*, 5204 – 5209.

[16] F. Niu, J. M. Liu, L. M. Tao, W. Wang, W. G. Song, *J. Mater. Chem. A* **2013**, *1*, 6130 – 6133.

[17] a) J. P. Malerich, K. Hagihara, V. H. Rawal, *J. Am. Chem. Soc.* **2008**, *130*, 14416 – 14417; b) R. I. Storer, C. Aciroa, L. H. Jones, *Chem. Soc. Rev.* **2011**, *40*, 2330 – 2346; c) Y. F. Wang, R. X. Chen, K. Wang, B. B. Zhang, Z. B. Li, D. Q. Xu, *Green Chem.* **2012**, *14*, 893 – 895; d) K. Bera, I. N. N. Namboothiri, *Chem. Commun.* **2013**, *49*, 10632 – 10634; e) J. H. Sim, C. E. Song, *Angew. Chem. Int. Ed.* **2017**, *56*, 1835 – 1839; *Angew. Chem.* **2017**, *129*, 1861 – 1865.

[18] X. Z. Bao, B. M. Wang, L. C. Cui, G. D. Zhu, Y. L. He, J. P. Qu, Y. M. Song, *Org. Lett.* **2015**, *17*, 5168 – 5171.

[19] a) J. Kaur, S. S. Chimni, S. Mahajana, A. Kumarb, *RSC Adv.* **2015**, *5*, 52481 – 52496; b) Q. He, L. Wu, X. Z. Kou, N. Butt, G. Q. Yang, W. B. Zhang, *Org. Lett.* **2016**, *18*, 288 – 291; c) M. Kumar, B. P. Kaur, S. S. Chimni, *Chem. Eur. J.* **2016**, *22*, 9948 – 9952.

[20] a) J. L. Figueiredo, M. F. R. Pereira, M. M. A. Freitas, J. J. M. Orfao, *Carbon* **1999**, *37*, 1379 – 1389; b) H. P. Boehm, *Carbon* **2002**, *40*, 145 – 149.

Manuscript received: November 28, 2017
Revised manuscript received: December 18, 2017
Accepted manuscript online: December 21, 2017
Version of record online: ■■ ▮▮, 0000

COMMUNICATIONS

L. Y. Zhao, X. Z. Bao, Q. T. Hu, B. M. Wang, A.-H. Lu**

■■ – ■■

Porous Carbon Nanosheet-Supported Chiral Squaramide for Highly Enantioselective Friedel–Crafts Reaction

Looking for support: A porous carbon nanosheet (PCN)-immobilized chiral catalyst is used in the asymmetric Friedel–Crafts addition of pyrazolones to isatin ketimines. The performance of the PCN-supported catalyst is comparable to that of its homogeneous catalyst; the products are obtained in high yields up to 90% with *ee* values as high as 99%. Recycling experiments confirm the stability of the catalyst.